

Capacity Analysis and Improvement for Coexisting IEEE 802.16 Systems in Unlicensed Spectrum*

Maciej Mühleisen
and Benedikt Wolz

Department of Communication Networks
Faculty 6, RWTH Aachen University, Germany
Email: [mue|bmw]@comnets.rwth-aachen.de

Mohammad M. Siddique
and Carmelita Görg

Communication Networks, TZI
University of Bremen, Germany
Email: [mms|cg]@comnets.uni-bremen.de

Abstract—Today spectrum demand for wireless communication is tremendous and even keeps growing. In contrast, there are no blank spots in the spectrum map. Additional spectrum opportunities are available in unlicensed bands and so-called non-exclusively licensed bands which are currently made available. This non-exclusive spectrum can be exploited whenever a license holder is not active.

These spectrum opportunities cannot be exclusively accessed so that multiple systems need to coexist. Existing MAC protocols need to be enhanced to allow a system to meet own Quality of Service (QoS) demands while allowing other coexisting systems to meet their QoS requirements.

In this work, methods for capacity calculation known from cellular networks are extended and applied to a scenario of coexisting IEEE 802.16 (WiMAX) systems. Developed methods are used to evaluate enhancements for interference mitigation which lead to increased capacity.

I. INTRODUCTION

Current and future cellular networks such as UMTS, LTE and IEEE 802.16 (WiMAX) are able to deliver contents with high data rates while guaranteeing sufficient QoS. This is possible since they operate on dedicated frequencies. Substantial prizes had to be paid by the operators to obtain licenses for the frequencies. Therefore operators plan and deployed the networks in a manner allowing to achieve best possible spectral efficiency.

High prizes and shortage of available spectrum have motivated novel licensing approaches. Besides bands dedicated to unlicensed operation, new spectrum opportunities are created through non-exclusive licensing. Here, systems are allowed to operate, if the license holder is not active. Systems operating in unlicensed and non-exclusively licensed bands cannot assume exclusive spectrum access. Multiple systems have to coexist and compete for spectrum access. Carrier Sensing (CS) is a technique commonly used for contention access in unlicensed spectrum. Unfortunately systems using CS experience unpredictable delays, increasing as the number of communicating nodes increases. Meeting QoS demands is not possible when CS is used. Therefore, novel contention protocols are required providing QoS in license-exempt bands. The challenge is to provide high data rates, low, predictable delays and fairness

in an environment with multiple, randomly deployed wireless systems.

IEEE 802.16 (WiMAX) is a centrally controlled, reservation based wireless protocol originally developed for cellular deployments in licensed bands. To make more spectrum available, methods are developed to enable WiMAX operation in license-exempt bands.

This paper is structured as follows: Section II presents a method to derive the Carrier to Interference Ratio (CIR) distribution of an arbitrary system deployment. Section III presents capacity results using this method. In section IV a Media Access Control (MAC) layer approach increasing capacity is presented. Section V concludes the paper.

A. IEEE 802.16 Frame Structure and Scheduler

The IEEE 802.16 (WiMAX) standard [1] defines a centrally controlled wireless communication protocol. A IEEE 802.16 network is formed of one or multiple Base Stations (BSs) and the associated Subscriber Stations (SSs). Each BS together with its associated SSs forms a cell. When operating in licensed bands, BS positions are planned by the operator. Two cases of unlicensed operation are possible: 1) a planned cellular system could operate in the same band as other cellular systems, for example from different operators, 2) it is also possible that WiMAX BSs are deployed by end-users as Wireless Local Area Network (WLAN) replacements. In both cases inter-cell distances and the number of interfering co-channel cells become random.

IEEE 802.16 systems follow a periodic frame structure as shown in Fig. 1. Each frame starts with a preamble followed by the Frame Control Header (FCH). Besides general information about the system, the FCH provides the first part of the so called Map. The Map is created by the scheduler defining the exact structure of the current frame. Therefore, it contains the information which node should transmit or receive at which point in time and which Modulation and Coding Scheme (MCS) is to be used.

For the downlink, the scheduler inspects the queue and possible MCS for each SS and grants each node an appropriate share of the frame, if possible. For the uplink, the scheduler relies on bandwidth requests from the SSs to estimate their demands. To select an appropriate MCS, the scheduler needs

*Founded by German Research Council (DFG) under GO 730/7-1 & WA 542/20-1

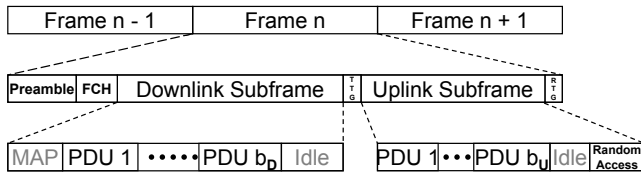


Fig. 1. IEEE 802.16 TDD frame structure.

channel state information such as estimated mean CIR or Packet Error Rate (PER).

B. Related Work

The IEEE standard draft 802.16h [2] proposes coexistence methods for 802.16 systems. One approach is to separate operation of several systems in time domain on the time scale of whole MAC frames. In [3] an approach is presented allowing multiple collocated 802.16 systems to coexist. Here systems are multiplexed in time domain on a time scale shorter than a MAC frame. The authors of [4] present methods for heterogeneous coexistence of IEEE 802.16 and IEEE 802.11 systems. Here busy tones are used preventing WLAN systems from channel access at times reserved for the WiMAX system.

In [5] the authors evaluate dynamic channel allocation algorithms for reservation in frame based communication systems similar to IEEE 802.16. They propose dividing the MAC frame into smaller time units called *Containers*. In the following this approach is evaluated analytically for coexisting IEEE 802.16 systems.

II. CIR DISTRIBUTION CALCULATION

In a planned cellular deployment, the distance D between two BSs operating on the same frequency channel can be assumed to be large compared to the cell radius R . Therefore, all co-channel interference can be modelled originating from the centre of the co-channel cells. In downlink mode, this is correct since power is emitted from the BSs in the centre of the cells. In uplink mode, this model is less precise with decreasing co-channel cell distance D . The authors of [6], [7] derived how to calculate the average interference power of a cell by integration over cell area. Here we want to extend this approach by calculating the CIR distribution experienced by a BS which receives a signal from a station at given distance d_C .

Firstly, only one interfering uplink transmission of an arbitrary SS in another cell is assumed. The resulting CIR of an uplink transmission of a SS in the evaluated cell can be calculated as $CIR = 10 \log_{10}(\frac{d_C^{-\gamma}}{d_I^{-\gamma}})$, with γ being the propagation factor, d_I the distance between interfering SS and evaluated BS, and d_C the distance between SS and BS in the evaluated cell. For k interferers the term $d_I^{-\gamma}$ becomes $\sum_{i=0}^k d_{I_i}^{-\gamma}$. Interference powers of SSs at equal distances d_I encounter the same path loss attenuation. The probability for a certain CIR is therefore directly related to the fraction of SSs in the interfering cell at distance d_I . As shown in Fig. 2, we

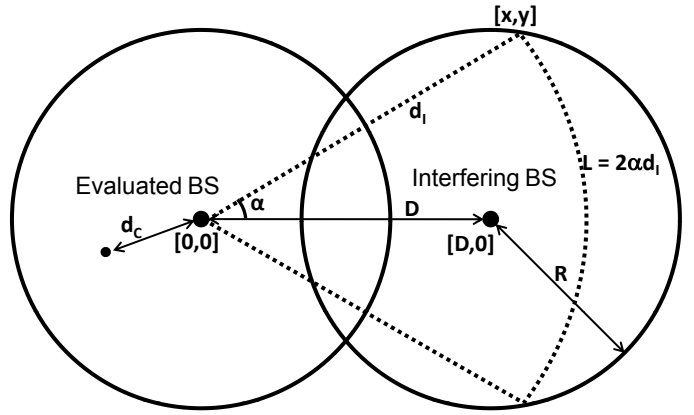


Fig. 2. Infinitesimal area of constant interference.

assume circle shaped cells. The left circle depicts the evaluated cell with the desired transmission from a SS at distance d_C . The right circle depicts the interfering cell. The dashed arc represents the infinitesimal thin area within which all SSs contribute to the same CIR. Its length is $2\alpha d_I$ limited by the cell boundary of the interfering cell. α can be calculated as $\alpha = \arctan(\frac{y}{x})$ with x, y being the coordinates of the crossing between the circle segment of distance d_I and the cell border of the interfering cell. The origin of the coordinate system is assumed at the BS of the evaluated cell. x and y are located at the circles with radius d_I and centre $[0, 0]$ and radius R with centre $[D, 0]$. The crossing point $[x, y]$ therefore has the coordinates:

$$x = \frac{D^2 - R^2 + d_I^2}{2D}, y = \sqrt{d_I^2 - x^2} \quad (1)$$

In assuming uniformly distributed SSs over the circle area of the interfering cell and by normalising to the cell area, the probability density function (PDF) of interference from a distance $D - R \leq d_I \leq D + R$ is given by:

$$p(d_I) = \frac{2d_I \arctan(\frac{y}{x})}{\pi R^2} \quad (2)$$

For unsynchronised systems, the downlink could be accounted for by increasing the probability $p(d_I = D)$ of interference from the centre of the interfering system where the interfering BS is located. For scheduling strategies other than round-robin, the distribution has to be adjusted accordingly.

The PDF of the distance dependant term of received interference power from one source $p(d_I^{-\gamma})$ can be calculated using following transformation:

$$p(I_i = d_I^{-\gamma}) = \frac{d_I^{\gamma+1}}{\gamma} p(d_I(I_i)) \quad (3)$$

with $d_I(I_i) = I_i^{-\frac{1}{\gamma}}$. The PDF of the sum of all interference

sources $I = \sum_{i=0}^k I_i$ can be obtained through convolution:

$$p(I) = \bigotimes_{i=0}^k p(I_i) = \bigotimes_{i=0}^k \frac{dI_i^{\gamma+1}}{\gamma} p(d_I(I_i)) \quad (4)$$

If SSs in the evaluated cells are also uniformly distributed, the PDF of the distance from the BS is:

$$p(d_C) = \frac{2d_C}{R^2} \quad (5)$$

The resulting CIR can be calculated as $CIR = -10\gamma \log_{10}(d_C) - 10 \log_{10}(I)$. Through transformation $d_C(C_{dB}) = 10^{-\frac{C_{dB}}{10\gamma}}$ and $I(I_{dB}) = 10^{-\frac{I_{dB}}{10}}$, the PDF of the logarithmic carrier and interference power C_{dB} and I_{dB} is determined by following expressions:

$$p(C_{dB}) = -\frac{d_C(C_{dB})}{10\gamma \ln(10)} p(d_C(C_{dB})) \quad (6)$$

$$p(I_{dB}) = -\frac{I(I_{dB})}{10 \ln(10)} p(I(I_{dB})) \quad (7)$$

The resulting CIR PDF is the convolution of (6) and (7):

$$p(CIR) = p(C_{dB}) * p(I_{dB}) \quad (8)$$

III. RESULTS

The presented formulas can be applied to an arbitrary number of interfering cells. To simplify matters, we show results for one interfering cell on one evaluated cell. A scenario where end-users put up IEEE 802.16 systems as WLAN replacements is assumed, so the cell size is set to $R = 50m$. The cell centre distance D is varied. In a real life scenario the distance D can take any arbitrary value caused by the positions of coexisting BSs. It is assumed that the evaluated cell has no impact on traffic statistics of the interfering cell.

Fig. 3 shows the resulting Cumulative Distribution Function (CDF) of the CIR for two different system distances D and propagation factors γ . If the systems are closer together, lower CIR values become more likely. This is obvious since the path loss attenuation of the interfering systems is lower at lower distances. A higher propagation factor leads to a better CIR since interference power is more affected by path loss than the carrier signal due to a larger link distance.

Table I shows the minimum CIR required for each MCS together with the resulting PHY data rate. For a distance of $D = 100m$ and a propagation factor of $\gamma = 4$, the probabilities for each MCS are shown in the most right column. If the CIR is below $6.4dB$, which is needed for the lowest MCS, communication is not possible. By weighting the PHY data rates for each MCS with the according probability and summing up, the total system capacity for the evaluated system can be calculated. Resulting capacity for this setup is $37.83Mbps$.

Fig. 4 shows the system capacities for increasing distances and different propagation factors. As expected, increasing the propagation factor increases system capacity. Since background noise is neglected, all SSs are able to use the highest

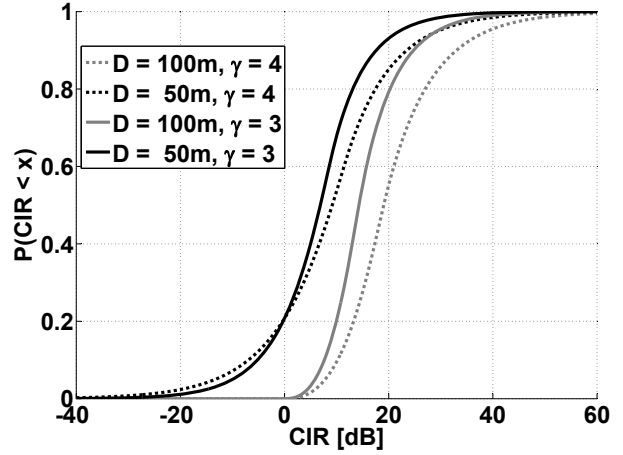


Fig. 3. CDF of CIR ($R = 50m$; $\gamma = 3, 4$; $D = 50m, 100m$).

TABLE I
IEEE 802.16 MCS

MCS	min. CIR [dB]	PHY Data Rate [Mbps]	Ratio
None	$-\infty$	0	2.9%
BPSK	6.4	6.91	5.0%
QPSK	9.4	13.82	4.7%
QPSK	11.2	20.74	21.7%
16QAM	16.4	27.65	10.2%
16QAM	18.2	41.47	22.3%
64QAM	22.7	55.30	5.9%
64QAM	24.4	62.21	27.3%

MCS from a certain distance on, leading to maximal capacity of $62.21Mbps$. In reality, transmission and noise power become the limiting factors once the interference from the other system can be neglected. Even at a distance of $0m$ when both systems cover the same area, communication is possible. In this case SSs close by the evaluated BS can still successfully be received if interfering SSs far from the BS are transmitting simultaneously. Here it is assumed that all SSs get an equal time share of the channel to assure fairness. Therefore, also a fraction of time is assigned to stations experiencing a CIR below $6.4dB$, resulting in a zero transmission rate. In reality, this fraction of time could be redistributed to other stations, but this is not considered in the results.

Still it is difficult for the scheduler in the BS to predict the CIR experienced by a SS. This is because the resulting CIR highly depends on which SS is active in the other system, which can not be influenced. Fig. 5 shows the CDF of the CIR of a SS at $d_C = 35m$ distance from its BS and propagation factor $\gamma = 4$. Results were derived analytically using formula (8) and by simulation with 100 and 1000 nodes. The measured CIR ranges from $6.2dB$ to $25.28dB$ which results from the minimum interfering distance $50m$ and maximum interfering distance $150m$. As expected, the simulation with 100 nodes shows significant differences to the analytic results but the trend and the limits match. With 1000 nodes results are

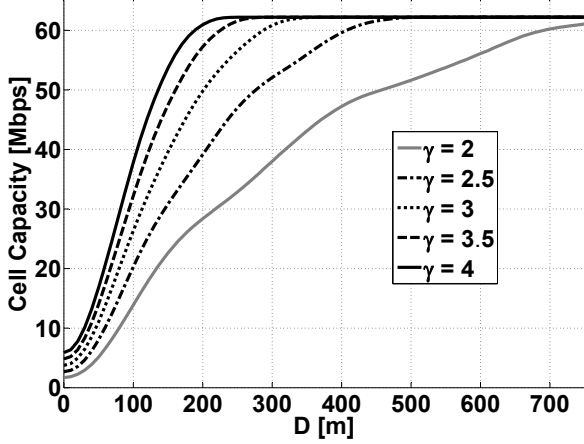


Fig. 4. System capacity for different distances D and propagation factors γ .

very close. The distance $35m$ is chosen because, assuming uniformly distributed SSs, approximately 50% of the stations are further away than $35m$ from the BS and the other half is closer. The CIR distribution ranges across all seven MCSs and even includes values too low for the most robust MCS (0.17%). If the scheduler uses the estimated mean value of past CIR measurements, $18.23dB$ is the calculated mean CIR. This corresponds to 16QAM 3/4 or, if mean CIR is underestimated a little, 16QAM 1/2 as MCS. Because of the high CIR standard deviation of $4.44dB$, experienced CIR is likely to differ from the mean value. With a 16% chance a better CIR can be selected. In this case resources are wasted because a higher data rate would be possible. Even worse is the fact that with a chance of 45.7% or 33.3% depending on whether 3/4 or 1/2 coding rate is chosen, the CIR is too low to successfully receive a transmission. A system can not operate at such a high error rate. The scheduler would have to rely on different measures than the mean CIR. It could for example observe the PER and keep choosing a more robust MCS until a certain mean PER is reached.

Fig. 6 shows the capacity for this rate adaptation algorithm compared with the case of optimal MCS selection from Fig. 4 for different PER values. The formula used to calculate the capacities is

$$C = (1 - PER) \int_0^R p(d_C) r_{max}(d_C, PER) dd_C \quad (9)$$

with $r_{max}(d_C, PER)$ being the rate of the maximal possible MCS at distance d_C not exceeding PER. $p(d_C)$ is calculated using formula (5). Retransmissions resulting from the PER are not accounted for. The capacity is significantly lower than the theoretic one when choosing the optimal possible MCS. For example at a distance $D = 100m$ capacity drops from $37.8Mbps$ to $17.11Mbps$ at 5% PER and $14.85Mbps$ at 2% PER. At distances up to $D = 180m$ the higher PER outperforms the lower one. This comes at the cost of a higher data loss.

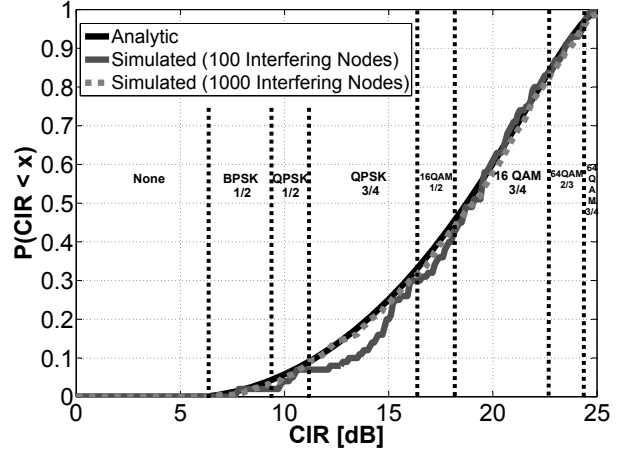


Fig. 5. CDF of the CIR for SSs at $d_C = 35m$ distance ($D = 100m$, $R = 50m$, $\gamma = 4$).

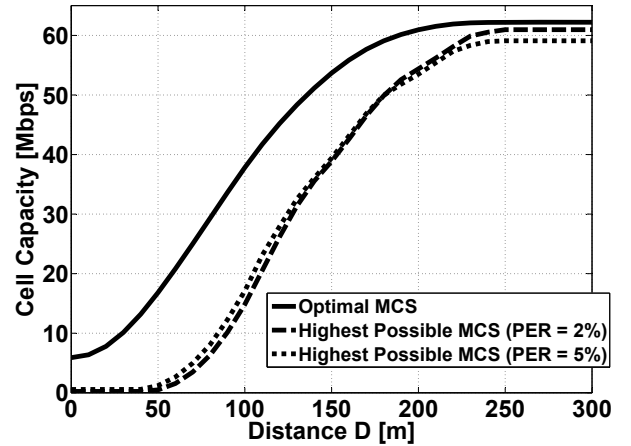


Fig. 6. Cell capacity if for every distance a MCS is chosen guaranteeing a certain PER ($R = 50m$, $\gamma = 4$).

IV. METHOD TO REDUCE THE CIR VARIANCE

In order to prevent packet loss, a too robust MCS must be chosen because of high variance and standard deviation of encountered CIR. As shown in Fig. 7, the standard deviation at a certain distance D between two cells grows with the size R of the interfering cell. At $100m$ distance the standard deviation is $6.89dB$ for an interfering cell size of $R = 50m$ which makes the selection of an MCS based on estimated mean CIR impossible. If the radius of the interfering cell is only $R = 12.5m$ the standard deviation is reduced to $1.09dB$ at $D = 100m$. Even at a distance of $D = 62.5m$, which assures the same minimal CIR as with a interfering cell of radius $R = 50m$, the standard deviation is only $1.74dB$. The length of the CIR intervals for each MCS reach from $1.7dB$ (64QAM 2/3) to $5.2dB$ (QPSK 3/4). The standard deviation for a cell radius of $12.5m$ could therefore be low enough to select a MCS based on estimated mean CIR.

Of course a simple reduction of cell sizes by keeping all SSs

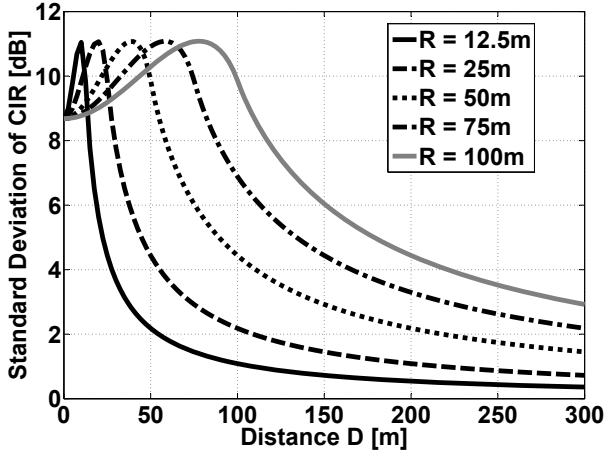


Fig. 7. Standard deviation of the CIR encountered by a SS at distance $d_C = 35m$ from the BS ($\gamma = 4$).

closer to the BS is not an option and would require more cells to cover the same area. Still, the same effect can be achieved by virtually reducing cell sizes through the MAC protocol. As shown in Fig. 8, each cell is divided into smaller areas. In this example the areas are shaped hexagonally. The MAC frame is divided into *containers* in time domain as done in [5]. For an Orthogonal Frequency Division Multiple Access (OFDMA) system this is done for every subchannel, as shown in Fig. 9. In reality a BS has to estimate the positions of its SSs and group them while assuring each SS belongs to a group and each group offers approximately the same traffic load. Methods to estimate SS position are beyond the scope of this work. Pattern recognition algorithms on measured CIR values could help to achieve this.

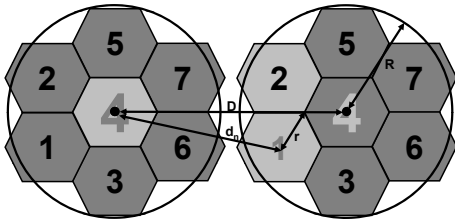


Fig. 8. Virtually reduced cell size by forming 7 hexagonal areas with radius $r = 2R/5$.

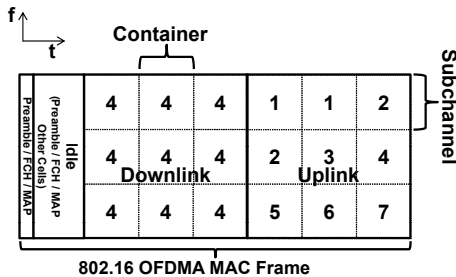


Fig. 9. Possible assignment of areas to MAC containers.

In every MAC container, only SSs from one area are active. It is possible to assign multiple containers to an area to deal with higher traffic demands. It is not possible to assign multiple areas to one container since this would increase interference variance. In this sample scenario, the evaluated cell has chosen an assignment as shown by areas of the same colour in Fig. 8. In reality the area-to-container assignment would be done by measuring each container and then selecting the best one in terms of mean CIR and variance. If the performance of a container degrades later on, an intra-cell-handover to a different container might be necessary. Analogous procedures can be found in the Digital Enhanced Cordless Telecommunications (DECT) standard [8].

Fig. 10 shows that a virtual reduction of the interfering cell size increases cell capacity. Capacity for each container is calculated using formula (9) but $p(d_C)$ is now calculated using formula (2) considering reduced virtual cell radius r and individual centre distance d_n for each area. It is assumed that the number of areas matches the number of containers. Therefore capacities for all areas are summed up and divided by the number of areas. Results are shown for 7 and 19 areas and compared with previous results for only one area. A random and a distance dependent area-to-container assignment is shown. For the random assignment 100 trials are generated to calculate a mean capacity for each distance. The distance dependent scheme assigns areas with high carrier signal to the same containers as close by interfering areas.

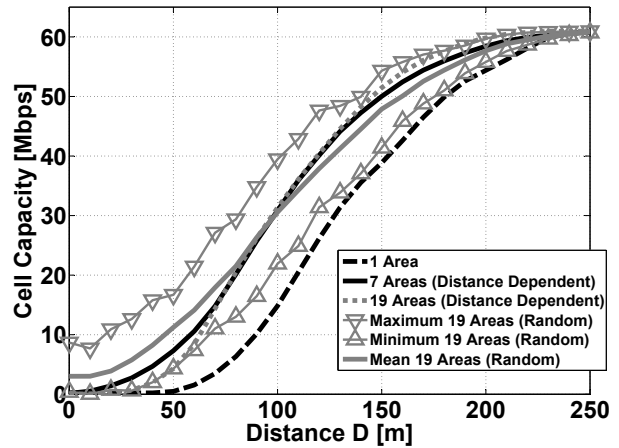


Fig. 10. Capacity with reduced virtual cell size ($PER = 2\%$, $R = 50m$; $r = 12.5m, 20m$, $R; \gamma = 4$).

Capacity with virtually reduced cell size is always higher than without. With distance dependant assignment, higher capacity is reached with 7 areas than with 19 at distances below 100m. 19 areas outperform 7 at distances above 100m. This is because for lower distances the cell areas begin to overlap. For such low interference distances, a better performance is achieved if areas with a high carrier signal are scheduled with areas of low interference, which is the opposite of chosen assignment scheme degrading 19 area performance more than 7 area performance. If cells are closer than 100m, capacity

is below half of the maximum. At distances that close it is better to use the IEEE 802.16h approach, separating cells in time domain giving each cell half of the capacity. Results for the random assignment do not show any difference in mean capacity for 7 (not shown) and 19 areas. The maximum gain is reached at 100m distance where capacity is doubled compared to one area. At this distance also the highest capacity range of around 17.5Mbps is encountered.

V. SUMMARY, CONCLUSION, AND OUTLOOK

A method was presented allowing multiple IEEE 802.16 systems to coexist in unlicensed frequency bands. Analytical results for the capacity of coexisting legacy IEEE 802.16 systems were derived and compared with the results for the proposed approach of virtually reduced cell size. The method shows a capacity gain of up to 100% from certain system distances on through spatial reuse. The drawback is that all systems have to follow the approach and that a method needs to be found to group SSs in the same area. Once this is assured, no changes to the IEEE 802.16 standard are required. The scheduling algorithm can be adjusted so that containers are established and areas are assigned to them. Also all systems need to provide sufficient idle periods for other systems to transmit their Preamble, FCH, and Map.

The presented analytic results show a gain and therefore motivate further research of this approach. A scenario with more than two cells will be evaluated analytically. Also further evaluation will be done using a system level IEEE 802.16 simulator. In this way, dynamic system properties including grouping of a finite number of SSs in areas, selecting the number of containers, areas-to-container assignment, mutual influence of all cells, and intra-cell-handover etc. can be accounted for.

ACKNOWLEDGMENT

The authors would like to thank Prof. Dr.-Ing. B. Walke for proposing the problem studied and for his support and friendly advice to this work.

REFERENCES

- [1] *IEEE Std 802.16-2004, IEEE Standard for Local and Metropolitan Area Networks. Part 16: Air Interface for Fixed Broadband Wireless Access Systems*, IEEE Std., 2004.
- [2] *IEEE Std 802.16h/D4, IEEE Standard for Local and Metropolitan Area Networks. Part 16: Air Interface for Fixed Broadband Wireless Access Systems. Improved Coexistence Mechanisms for License-Exempt Operation*, IEEE Std., Feb 2008.
- [3] M. Muehleisen, R. Jennen, M. Siddique, and C. Goerg, "IEEE 802.16 Coexistence through Regular Channel Occupation," in *Proceedings of European Wireless Conference 2009*, Aalborg, Denmark, Jun 2009.
- [4] L. Berlemann, C. Hoymann, G. Hiertz, and B. Walke, "Unlicensed Operation of IEEE 802.16: Coexistence with 802.11 (A) in Shared Frequency Bands," *Proc. of PIMRC 2006*, pp. 1–5, 2006.
- [5] A. Krämling, M. Scheibenbogen, and B. Walke, "Dynamic channel allocation in wireless ATM networks," *Wireless Networks*, vol. 6, no. 5, pp. 381–389, 2000.
- [6] C. Hoymann and S. Goebbels, "Dimensioning Cellular WiMAX Part I: Singlehop Networks," in *Proceedings of 13th European Wireless Conference, 2007*.
- [7] J. Habetha and J. Wiegert, "Network capacity optimisation, Part 1: cellular radio networks," in *Proceedings of 10th Symposium on Signal Theory, Aachen*, 2001, pp. 125–132.
- [8] H. Eriksson and R. Bownds, "Performance of dynamic channel allocation in the DECT system," in *41st IEEE Vehicular Technology Conference, 1991. Gateway to the Future Technology in Motion.*, 1991, pp. 693–698.